AD-A089 906 DEFENCE RESEARCH ESTABLISHMENT VALCARTIER (QUEBEC) F/G 20/5
A ONE-DIMENSIONAL NUMERICAL MODEL OF LASER HEATING OF TARGET SL--ETC(U)
MAY 80 J P MORENCY
UNCLASSIFIED DREV-R-4166/80 NL

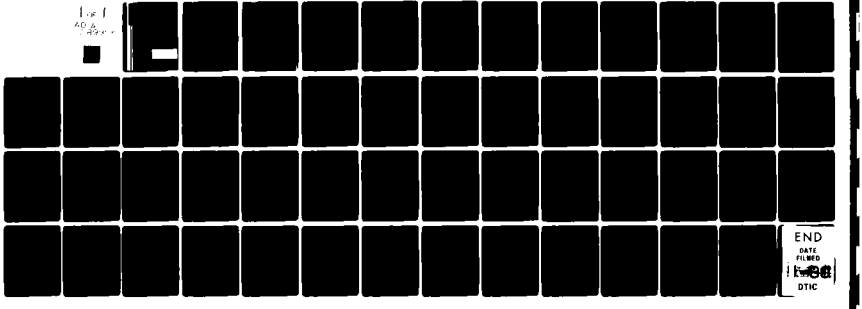

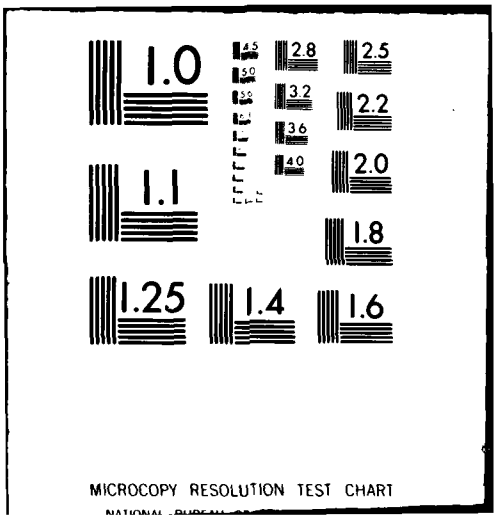
1.0
1.1
1.25
1.4
1.6
1.8
2.0
2.2
2.5
2.8
3.2
3.6
4.0
4.5
5.0
MICROCOPY RESOLUTION TEST CHART

UNCLASSIFIED
UNLIMITED DISTRIBUTION

CRDV RAPPORT 4166/80
DOSSIER: 3633B-006
MAI 1980

DREV REPORT 4166/80
FILE: 3633B-006
MAY 1980

A ONE-DIMENSIONAL NUMERICAL MODEL OF LASER HEATING OF TARGET SLABS

J.P. Morency

Centre de Recherches pour la Défense
Defence Research Establishment
Valcartier, Québec

BUREAU - RECHERCHE ET DEVELOPPEMENT
MINISTERE DE LA DEFENSE NATIONALE
CANADA

NON CLASSIFIÉ
DIFFUSION ILLIMITÉE

RESEARCH AND DEVELOPMENT BRANCH
DEPARTMENT OF NATIONAL DEFENCE
CANADA

CRDV R-4166/80
DOSSIER: 3633B-006

UNCLASSIFIED

(14) DREV-R-4166/80
FILE: 3633B-006

(11) May 80

(12) 52

(6) A ONE-DIMENSIONAL NUMERICAL MODEL
OF LASER HEATING OF TARGET SLABS
(Un modèle Numérique Unidimensionnel du Chauffage d'une Plaque Metallique par Laser)

J.P. Morency

(10) J.P. Morency

CENTRE DE RECHERCHES POUR LA DEFENSE
DEFENCE RESEARCH ESTABLISHMENT
VALCARTIER
Tel: (418) 844-4271

Quebec, Canada

May/mai 1980

NON CLASSIFIE

RESUME

Dans ce rapport on développe un schéma numérique de solution de l'équation unidimensionnelle non linéaire de conduction de la chaleur. On applique ensuite ce schéma à l'interaction laser-métaux et on montre l'importance de la variation des propriétés thermophysiques sur la distribution de la température dans une plaque métallique. (NC)

ABSTRACT

This report establishes a numerical scheme to solve the nonlinear one-dimensional heat transfer equation. The scheme is then applied to the case of laser-metals interaction and used to show the importance of thermophysical properties variation on the temperature distribution within a slab. (U)

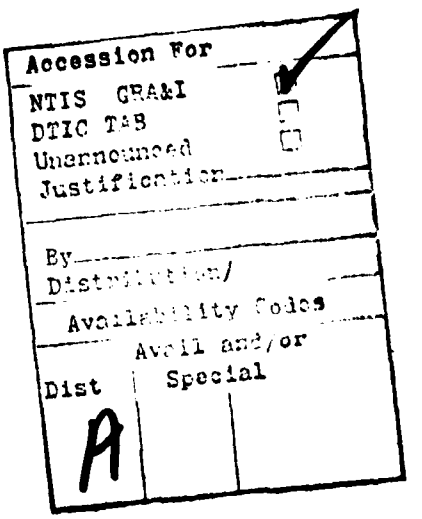

TABLE OF CONTENTS

1.0 INTRODUCTION

The development of the CO_2 laser with its high efficiency and high output power has made possible a variety of laser-target interaction experiments. However, as the cost of performing exhaustive parametric studies to establish potential applications is prohibitive, computer simulations were developed which can predict laser effects with sufficient accuracy to reduce the number of required experiments to an acceptable level.

Although Hanley (Ref. 1) has developed an operational finite difference code to solve the three-dimensional heat flow equation, his solution does not conserve energy and leads to inaccurate results. For simplicity, in this report, we solve the one-dimensional problem by properly treating the boundary conditions to conserve energy. Exploitation of the Kirchhoff transformation of the temperature scale allows temperature-dependent physical properties to be included relatively simply. Furthermore, by reducing the truncation error to terms of second order in time and fourth order in space, we obtain significantly more accurate results for a specific time or, conversely, we reduce the computation time for a given accuracy. The extension of this numerical scheme to three-dimensional problems is straightforward.

Section 2 deals with the mathematical formulation of the problem, and Section 3 develops the finite-difference approach used to solve the one-dimensional heat diffusion equation. In Section 4, we present some numerical results and compare them with the few existing analytical solutions. In Section 5, we discuss our results and their limitations.

This work was performed at DREV between May 1978 and February 1979 under PCN 33B06, Effects of Laser Beams on Materials.

2.0 FORMULATION OF THE PROBLEM

The mathematical treatment of laser-target interaction involves the solution of the differential equation of heat conduction in bounded media under appropriate initial and boundary conditions. For a stationary, homogeneous, isotropic solid with internal heat generation the differential equation in a Cartesian coordinate is (Refs. 2, 3)

$$\rho\, C_p(T)\, \frac{\partial T}{\partial t}\,(z,t) = \frac{\partial}{\partial z}\left[K(T)\ \frac{\partial T}{\partial z}\ (z,t)\right] + g[z,t] \qquad [1]$$

In this equation, ρ is the density, C_p, the specific heat at constant pressure, T, the temperature, z, the spatial coordinate, t, the time, K, the thermal conductivity and g[z,t], the internal heat source or sink.

This differential equation of heat conduction has numerous solutions, unless a set of suitable boundary and initial conditions are prescribed. In this study, we consider linear and nonlinear boundary conditions of the first and second kind. Mathematically, they have the following forms:

$$T = T_o \text{ or } 0 \qquad [2a]$$

and/or

$$K[T]\ \frac{\partial T}{\partial \eta_i} = F \qquad [2b]$$

where T_o is a constant temperature, $\partial/\partial\eta_i$ denotes differentiations along the outward-drawn normal at the boundary surface, S_i, and F can be arbitrary functions of time and surfaces.

When the thermal properties of the solid vary with temperature, the partial differential equation is nonlinear. If it is assumed

that ρ, C_p and K are dependent on temperature but independent of position and time, and that the heat-generation term $g \equiv g(z,t)$ is independent of temperature, then, changing the dependent variable using the Kirchhoff transformation (Refs. 2,4,5) will remove the thermal conductivity from the differential operator.

This transformation is accomplished by defining a new dependent variable, U, as

$$U = \int_{o}^{T} \frac{K(T')}{K_o} \, dT' \qquad [3]$$

where $U \equiv U(T)$, $T \equiv T(z,t)$ and K_o is the value of thermal conductivity for $T = 0$. Since K is a function of T only eq. 1 can be written in the following form

$$\rho C_p \frac{\partial T}{\partial t} = K \frac{\partial^2 T}{\partial z^2} + \frac{\partial K}{\partial z} \cdot \frac{\partial T}{\partial z} + g \qquad [4]$$

Expressing $\frac{\partial K}{\partial z}$ in the form

$$\frac{\partial K}{\partial z} = \frac{dK}{dT} \cdot \frac{\partial T}{\partial z} \qquad [5]$$

and substituting this into eq. 4 gives

$$\rho C_p \frac{\partial T}{\partial t} = K \frac{\partial^2 T}{\partial z^2} + \frac{dK}{dT} \left(\frac{\partial T}{\partial z}\right)^2 + g \qquad [6]$$

From eq. 3 we find

$$\frac{\partial U}{\partial t} = \frac{du}{dT} \cdot \frac{\partial T}{\partial t} = \frac{K}{K_o} \frac{\partial T}{\partial t} \qquad [7a]$$

$$\frac{\partial U}{\partial z} = \frac{dU}{dT} \cdot \frac{\partial T}{\partial z} = \frac{K}{K_o} \frac{\partial T}{\partial z} \qquad [7b]$$

$$\frac{\partial^2 U}{\partial z^2} = \frac{\partial}{\partial z} \frac{K}{K_o} \frac{\partial T}{\partial z} = \frac{1}{K_o} \frac{\partial K}{\partial z} \cdot \frac{\partial T}{\partial z} + K \frac{\partial^2 T}{\partial z^2} \qquad [7c]$$

Substituting eq. 7 in eq. 6 gives

$$\frac{1}{\alpha} \frac{\partial U}{\partial t} = \frac{\partial^2 U}{\partial z^2} + \frac{g}{K_o} \qquad [8]$$

Since the thermal diffusivity $\alpha = K/\rho C_p$ in eq. 8, is a function of temperature, the equation is still nonlinear, but simpler in form. Through this transformation, the boundary conditions become

$$U = U_o \qquad [9a]$$

and/or

$$K_o \frac{\partial U}{\partial \eta_i} = F \qquad [9b]$$

Even with these simplifications, the solution of the differential equation is very complex and analytical results can only be obtained for a restricted number of particular or specific cases, which we will use without derivation to check the valicity of our numerical model. Following Hanley (Ref. 1), we use a standard finite-difference approximation to solve this one-dimensional heat conduction equation. One of

our aims is to obtain a good compromise between computer time and accuracy of the results, particularly those related to a comparison with experimental ones.

3.0 FINITE-DIFFERENCE MODEL

3.1 Finite-Difference Approximation

We use an explicit, central difference scheme to solve the following differential equation:

$$\frac{\partial U}{\partial t}(z,t) = \frac{\alpha \partial^2 U}{\partial z^2}(z,t) + \frac{\alpha g}{K_o} \qquad [10]$$

We consider only materials opaque to the incident laser beam (i.e. materials such as metals for which the absorption depth is much less than the wavelength of the laser radiation) and chemically as well as nuclearly stable. Under such circumstances, there is no internal heat source or sink and, therefore, $g(z,t) = 0$.

The boundary-value problem under consideration is that of a slab of finite thickness whose front surface has a uniform and constant thermal load (i.e. $\partial U/\partial z = Cte$ at $z = 0$), whereas the back surface is either insulated (i.e. $\frac{\partial U}{\partial z} = 0$ at $z = L$) or held at the ambient temperature (i.e. $U = U_o$ at $z = L$).

We use a Taylor series expansion of the function as our basic concept in the finite-difference approximation of the differential equation and the related boundary conditions. Since the procedure is

quite straightforward, we will give only the main results here. When a function U(z,t) and its derivatives are finite, continuous, and have a single value, this function can be expanded in the form of the Taylor series about the point z as

$$U(z+\Delta z,t) = U(z,t) + \Delta z. \frac{\partial U}{\partial z}(z,t) + \frac{\Delta z^2}{2!} \frac{\partial^2 U}{\partial z^2}(z,t) + \frac{\Delta z^3}{3!} \frac{\partial^3 U}{\partial z^3}(z,t) + \ldots \quad [11]$$

or

$$U(z-\Delta z,t) = U(z,t) - \Delta z. \frac{\partial U}{\partial z}(z,t) + \frac{\Delta z^2}{2!} \frac{\partial^2 U}{\partial z^2}(z,t) - \frac{\Delta z^3}{3!} \frac{\partial^3 U}{\partial z^3}(z,t) + \ldots \quad [12]$$

The first-order central-difference approximation is obtained by subtracting eq. 12 from eq. 11

$$\left.\frac{\partial U}{\partial z}(z,t)\right]_z = \frac{U(z+\Delta z,t) - U(z-\Delta z,t)}{2\Delta z} + O(\Delta z^2) \quad [13]$$

The term $O(\Delta z^2)$ on the right-hand side indicates that the error involved in cutting off the infinite series is of the order of (Δz^2). Similarly, the addition of eqs. 11 and 12 gives the second derivative of the function as

$$\left.\frac{\partial^2 U}{\partial z^2}(z,t)\right]_z = \frac{U(z+\Delta z,t) + U(z-\Delta z,t) - 2U(z,t)}{\Delta z^2} + O(\Delta z^2). \quad [14]$$

where the truncation error is of the order of (Δz^2).

We also have for the time variable the following finite-difference approximation

$$\left.\frac{\partial U}{\partial t}(z,t)\right]_t = \frac{U(z,t+\Delta t) - U(z,t)}{\Delta t} + O(\Delta t) \qquad [15]$$

We then find, for the finite-difference approximation, the following relation

$$U(R,\ell+1) = U(R,\ell) + \frac{\alpha\Delta t}{[\Delta z]^2}\left[U(R+1,\ell) + U(R-1,\ell) \right] - \frac{2\alpha\Delta t}{[\Delta z]^2} \cdot U(R,\ell) + O(\Delta t) + O(\Delta z^2) \qquad [16]$$

where Δz is the spatial increment and Δt, the temporal one; R refers to lattice points along the z axis and ℓ, to the integral multiple of the step Δt along the time axis. The coefficient α is the temperature-dependent thermal diffusivity and can be expressed as

$$\alpha(T) = \frac{K(T)}{\rho(T) \cdot C_p(T)} \qquad [17]$$

3.2 Boundary Conditions

Using the central-difference approximation, the boundary conditions become

1. Back surface

   a) Held to ambient

   $$U(Rmax, \ell) = U_o \qquad [18a]$$

   b) Insulated (i.e., no heat flow)

   $$U(Rmax. + 1, \ell) = U(Rmax. -1, \ell) \qquad [18b]$$

and

2. Front surface

$$U(Rmin. - 1,\ell) = U(Rmin. + 1,\ell) + \frac{2\Delta z}{K_o}. \quad \varepsilon\ (T)\ .\ \phi\ .\ COS\ \theta \quad [19]$$

where Rmax. and Rmin. indicate respectively the maximum and the minimum values on the z axis, K_o is the ambient temperature thermal conductivity, $\varepsilon(T)$ the temperature-dependent absorption or coupling coefficient, ϕ, the incident flux or power density on the material and θ, the angle of incidence of the laser beam with respect to the normal to the front surface.

3.3 Errors Involved in Finite Differences

Since in the process of the numerical solution of differential equations the derivatives are approximated with finite-difference expressions at each nodal point, an analysis of the possible errors involved and of the way to reduce them is paramount. There are two main types of errors: round-off and truncation errors. Furthermore, because of the explicit numerical scheme used, a specific relation between the spatial and the temporal variables must be satisfied. This relation is called the stability criterion. A detailed derivation of the results given below is beyond the scope of the present work. However, interested readers can consult, for more information, anyone of the following publications (Refs. 6-9).

3.3.1 Round-Off Errors

Numerical calculations are carried out only to a finite number of significant figures. At each step, the error introduced by rounding off the numerical calculations is called the round-off error. In linear problems, the effects of these errors superimpose themselves in the

solution. The use of small mesh size, although desirable for a better approximation of the differential equation, increases the cumulative effect of round-off errors. Therefore, one cannot always say that decreasing the mesh size necessarily increases the accuracy in finite-difference calculations. On the other hand, carrying out the numerical calculations at the intermediate stages to two or more additional significant figures will reduce the cumulative effect of round-off errors at the expense of increasing the computation time. However, since the distribution of these errors has many of the features of a random process, it is likely that the effects of these errors will generally cancel each other in part. Therefore, it is very difficult to determine exactly the order of magnitude of the cumulative departure of the solution due to round-off errors.

3.3.2 Stability of Finite-Difference Solutions

At each stage of the calculations, some round-off errors will be present. The solution of finite-difference equations is called stable if the difference between the exact and the numerical solutions tends to zero as Δt and Δz tend to zero and does not increase exponentially. Specifically, the solution will be stable if the following condition is satisfied:

$$2\,\alpha.\Delta t\left[\frac{1}{(\Delta z)^2}\right] \leq 1 \qquad [20]$$

It should be noted that the form of the difference equations depends on the type of the differentiation scheme used, that of differential equations and the boundary conditions. Therefore, the stability criteria given above cannot be generalized for other systems. In fact, each system must be examined individually for stability.

Unfortunately, there is no general method, for nonlinear problems, that can be used effectively to determine the stability of the resulting finite-difference equation.

3.3.3 Truncation Error

The Taylor series expansion, used in expressing a partial differential equation in finite differences, is truncated after a prescribed number of terms. The error involved in each step of calculation resulting from the truncation of the series is called the truncation error. In our case, that error involves terms of order Δt and $(\Delta z)^2$. As the mesh size is reduced, and accordingly the time step to satisfy the stability criteria, the truncation error is expected to become smaller so that the numerical solution converges faster to the true solution. Of course, this increases the number of nodal points and the computation time. It is interesting to note that the truncation error is reduced to terms of order $(\Delta t)^2$ and $(\Delta z)^4$ by satisfying the following relation:

$$\alpha.\Delta t\left[\frac{1}{(\Delta z)^2}\right] = \frac{1}{6} \qquad [21]$$

Under this condition, the finite-difference solution approaches, within a determined residual error, the true solution of the differential equation at a faster rate and it will be used in our numerical scheme. This value is called the "stability constant" and it will be referred to under this name later on.

3.4 Program Summary

A computer program has been written in FORTRAN IV to evaluate the finite-difference approximation described in the previous section. A listing appears in Appendix A along with detailed running instructions.

The program can deal with different types of opaque materials as long as their thermophysical properties and their temperature variation are known. The number of points in the lattice along the z axis is variable to permit the user to satisfy specific needs.

In addition, an analytical solution calculation for constant thermophysical properties has been introduced into the program to check the numerical results. Finally, the user can obtain the temperature distribution as a function of time in tabular and graphical forms.

4.0 RESULTS

4.1 Analytical Solutions

Schriempf (Ref. 10) gives analytical solutions to the heat diffusion equation in the one-dimensional situation. He assumes the laser beam is constant and uniform, the material parameters are temperature independent, the solid is uniform and isotropic. Furthermore, there are no internal heat sources or sinks, and no phase change in the materials is considered.

The solution for the semi-infinite solid is

$$T(z,t) = \frac{2.\,\varepsilon.\,\phi.\,\cos\theta}{K}\,.\sqrt{\alpha t}\,.\,\mathrm{ierfc}\left[\frac{z}{2\sqrt{\alpha t}}\right] \qquad [22]$$

and

$$T(0,t) = \frac{2.\varepsilon.\phi.\,\cos\theta}{K}\,.\sqrt{\frac{\alpha t}{\pi}} \qquad [22a]$$

Similarly, the solution for a slab of finite thickness is

$$T(z,t) = \frac{\varepsilon.\phi.\ (\cos\theta).L.}{K}\left\{\frac{\alpha.t}{L^2} + \left[\frac{3\ (L-z)^2 - L^2}{6L^2} - \frac{2}{\pi^2}\sum_{n=1}^{\infty}\frac{(-1)^n}{n^2}\ .\ e^{-\alpha n^2\pi^2 t/L^2}\ .\left(\cos\frac{n\pi(L-z)}{L}\right)\right]\right\} \quad [23]$$

and

$$T(0,t) = \frac{\varepsilon.\phi.\ (\cos\theta).\ L.}{K}\left\{\frac{\alpha.t}{L^2} + \left[\frac{1}{3} - \frac{2}{\pi^2}\sum_{n=1}^{\infty}\frac{1}{n^2}\ .e^{-\alpha n^2\pi^2 t/L^2}\right]\right\} \quad [23a]$$

where L is the slab thickness, and the condition for an insulated back surface is

$$\left.\frac{\partial T}{\partial z}\right)_{z=L} = 0 \quad [24]$$

Equation 23 has been included into the program appearing in Appendix A, such that the reliability of the numerical results, for similar conditions, can be assessed.

4.2 Numerical Solutions

The numerical results obtained in calculating the function U are identical to those of the temperature T, if we assume that the thermophysical properties are temperature independent. Otherwise, we have to solve the following equation

$$U(T) = \frac{1}{K_o}\int_{o}^{T} K(T')\ dT' \quad [25]$$

to find the temperature distribution through the slab considered. For metals studied here, the thermal conductivity of the solid phase is

$$K(T') = K_o \quad (1 + \beta T') \qquad [26]$$

Substituting eq. 26 into eq. 25 gives

$$U = T + \frac{\beta}{2} \; T^2 \qquad [27]$$

and finally,

$$T = \frac{1}{\beta} \left[\sqrt{1 + 2.\beta.U(z,t)} \; - 1 \right] \qquad [28]$$

Furthermore, we assume that the thermal diffusivity is as follows:

$$\alpha(T') = \frac{K(T')}{\rho_o \, C_p(T')} = \frac{K_o(1 + \beta T')}{\rho_o C_{p_o} \, (1 + \gamma T')} \qquad [29]$$

where K_o is the thermal conductivity, ρ_o, the density (assumed constant in the temperature range considered) and C_{p_o}, the specific heat at the initial temperature (i.e. room temperature in our case).

4.2.1 Numerical vs Analytical Solutions

This section compares the numerical and the analytical solutions for similar conditions; it also gives an assessment of the accuracy and reliability of our numerical model.

Figure 1 shows the analytical solution (alternating lines) and the numerical results (continuous lines), with temperature independent thermophysical properties, for a 6-node case (i.e. $\Delta z = 0.2$ cm) along the z axis. Each curve represents the temperature distribution at 5 time step increments (i.e. $5\Delta t$). Both models predict the same front surface temperature, within 1%, after only 25 time steps (25 Δt) or about 0.2 s in the present case. Furthermore, if we calculate, for a specific time, the area under each curve we obtain the same result, which demonstrates that we satisfy the energy conservation principle.

The same results appear in Fig. 2, but for a 21-node case (i.e. $\Delta z = 0.05$ cm) along the z axis. Each curve corresponds to 16 time steps. Except for the first few curves, it is very difficult to differentiate between the results. As a matter of fact, we have, within 0.5%, similar results on the front surface after only 16 time steps or about 0.006 s in this case. However, this accuracy was obtained at the expense of increasing the computation time by a factor of 64. This is because Δz is 4 times smaller and Δt is 16 times smaller since $\Delta t \propto (\Delta z)^2$.

This demonstrates that the numerical solution can give, with some compromise, results comparable to those of the analytical one. In the next section, the numerical solution is applied to cases where no analytical solutions exist, but where there are a few approximate ones.

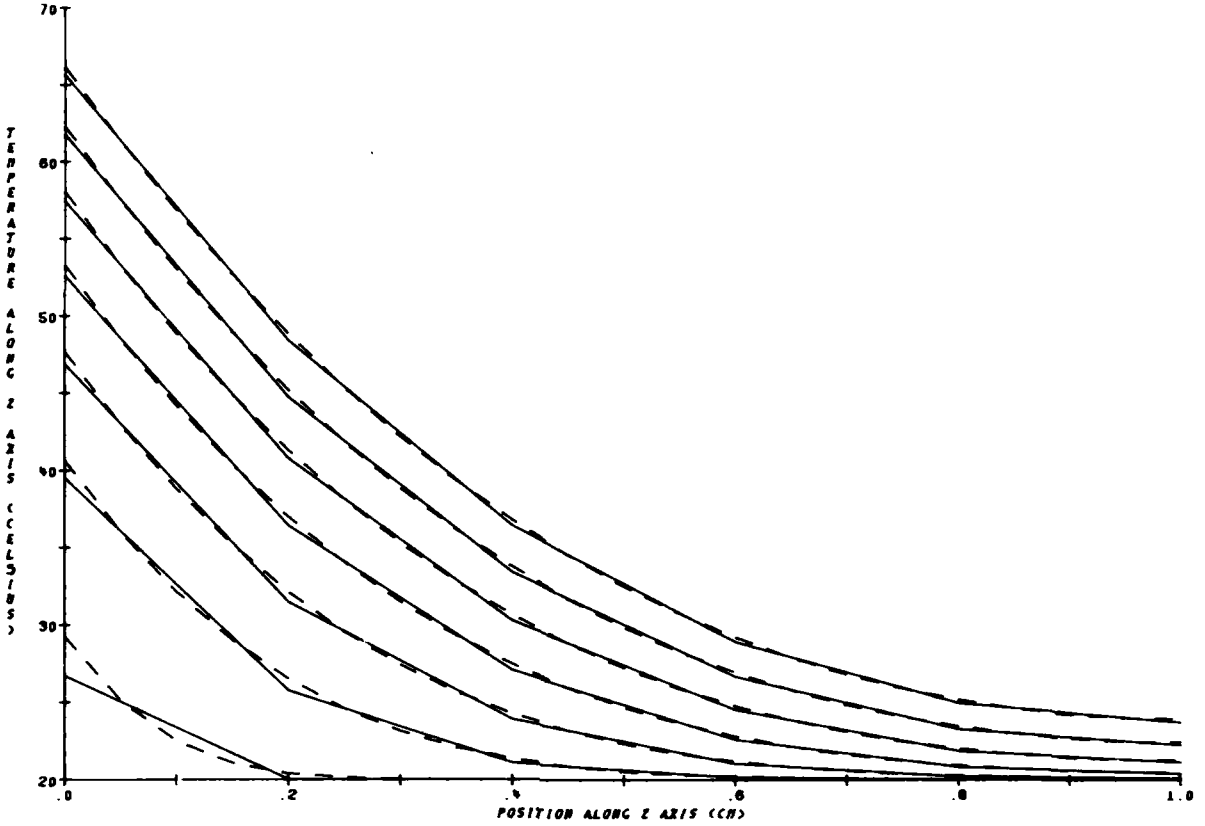

FIGURE 1 - Temperature distribution within a 1 cm-thick Cu target for an incident intensity of 2,000 W/cm^2 and a coupling coefficient of 0.02. Each curve corresponds to 5 time increments (5 Δt) of the numerical solution. The continuous lines represent the temperature independent thermophysical properties numerical case (6 nodes along z axis) whereas the alternating lines show the analytical solution.

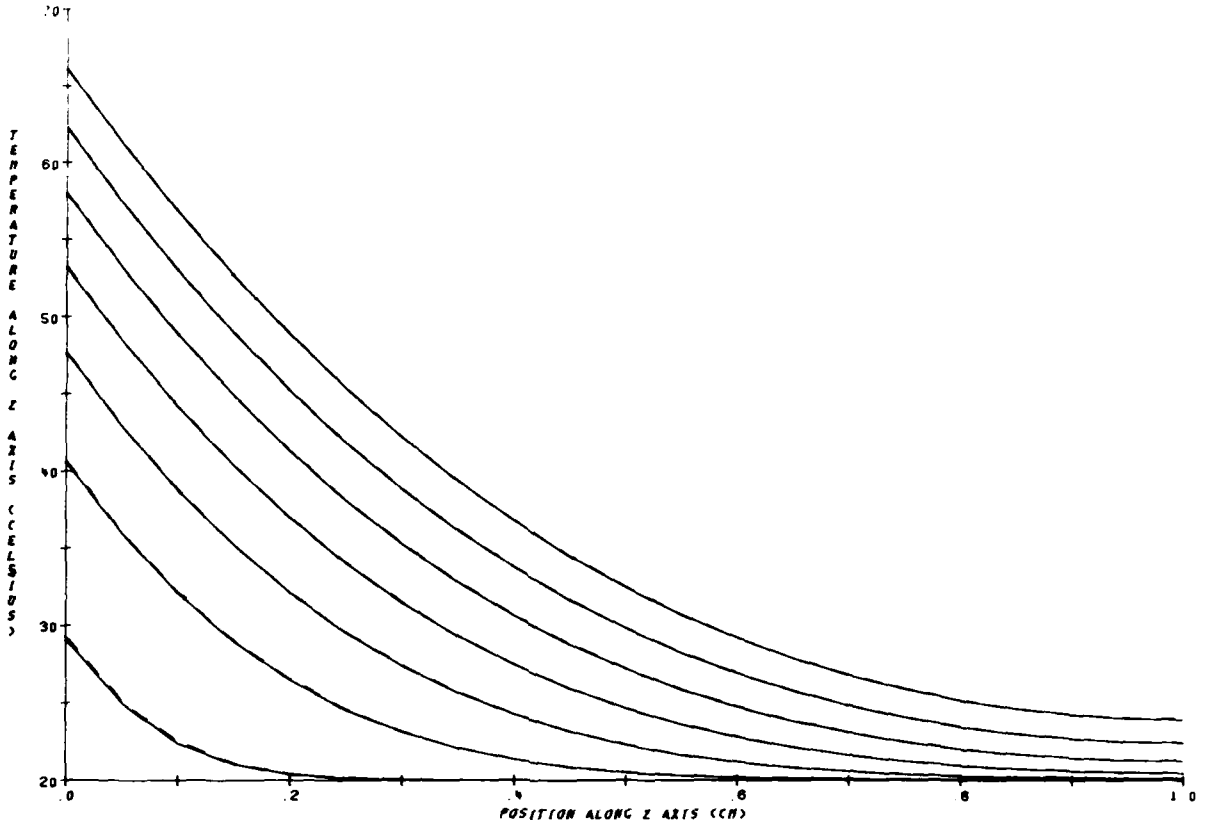

FIGURE 2 - Similar to Fig. 1 but for 21 node numerical case. Each curve corresponds to 16 time increments (16 Δt).

4.2.2 Temperature-Dependent Thermophysical Properties

The temperature dependence of thermophysical properties is an important factor in dealing with laser-matter interactions. Figure 3 shows some results for copper with 6 nodes along the z axis. We have assumed that the thermophysical properties vary linearly with temperature. The continuous curves represent the temperature-dependent results while the alternating curves are the results for the constant room-temperature case. The time interval between curves is 0.25 s. Both temperature distributions are similar at 0.25 s but quite different after 4.5 s. We calculate an error of 10% or about 0.5 s of the total time to reach melting on the front surface between the two models. In other words, it takes 0.5 s longer to reach melting on the front surface, for the specified conditions, if you consider temperature-dependent properties as in the physical world.

Figure 4 shows the absolute error in temperature for the preceding conditions. The error increases from the front to the back surface. These results indicate a decrease in the thermal diffusivity of copper with temperature as expected (Ref. 11). Figure 5 presents the relative error in percentage for the same conditions.

Figure 6 illustrates the results obtained for stainless steel # 304. This case demonstrates the drastic influence of the temperature-dependent thermophysical properties. Under the present conditions, there is a twofold increase in the time required to reach melting on the front surface between the two models. In the variable model, melting on the front surface can be reached in 3 s, whereas in the constant model, this can be achieved within 1.5 s.

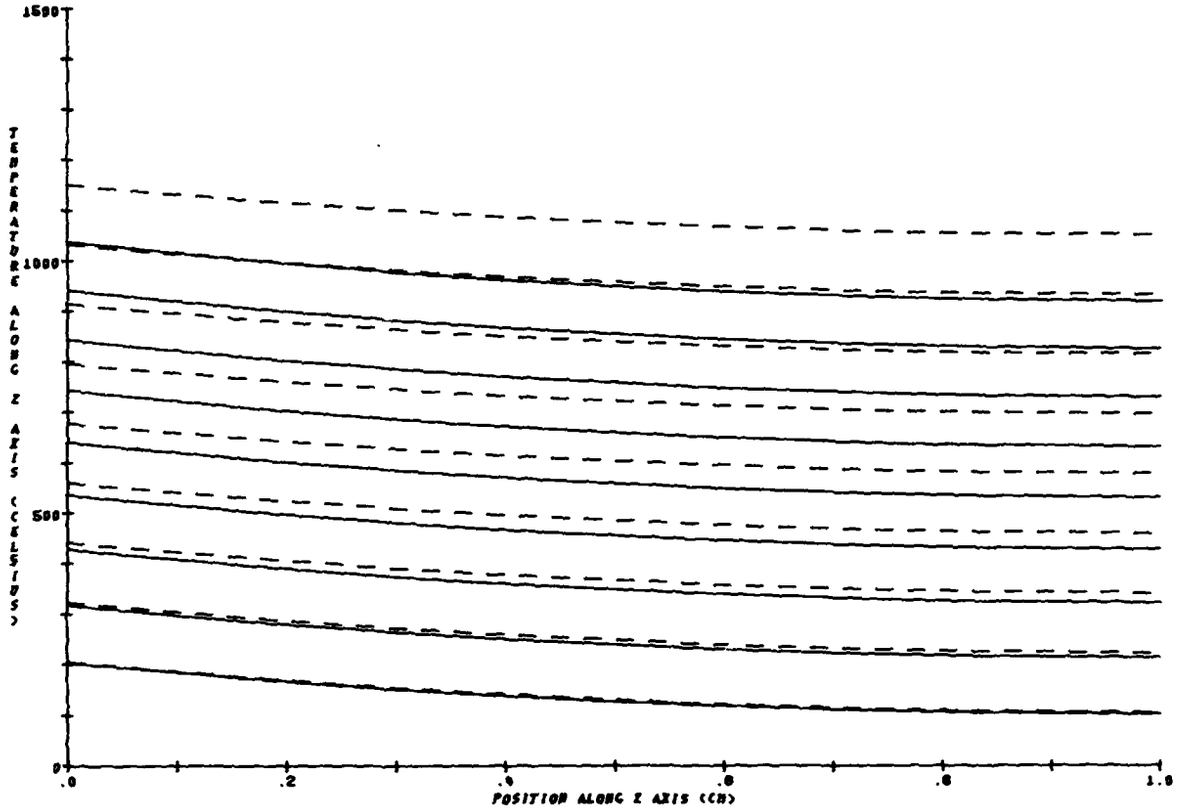

FIGURE 3 - Temperature distribution within a 1 cm-thick Cu target (6 nodes along z axis) for an incident intensity of 20,000 W/cm^2 and a coupling coefficient of 0.04. The time interval between each curve is 0.25 s for the temperature-dependent case (continuous lines) and for the constant room-temperature case (alternating lines).

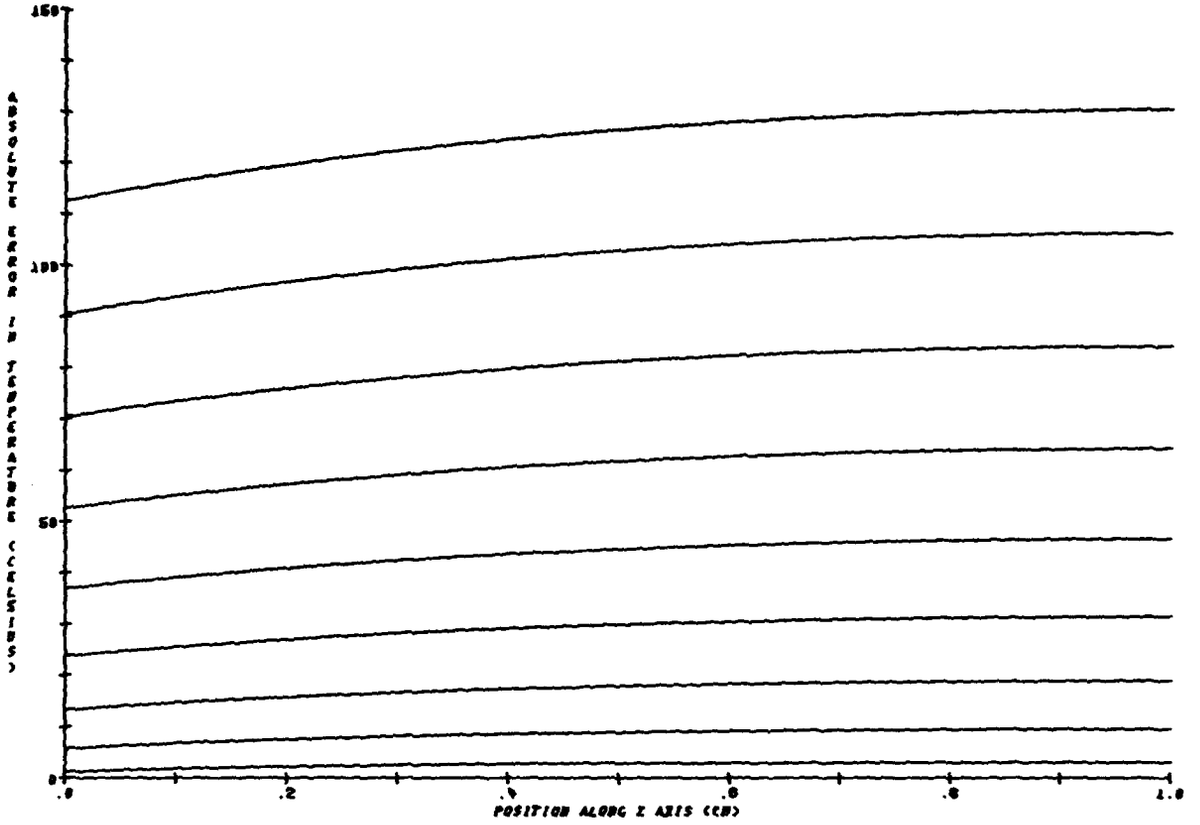

FIGURE 4 - Absolute error in temperature distribution between the two models of Fig. 3.

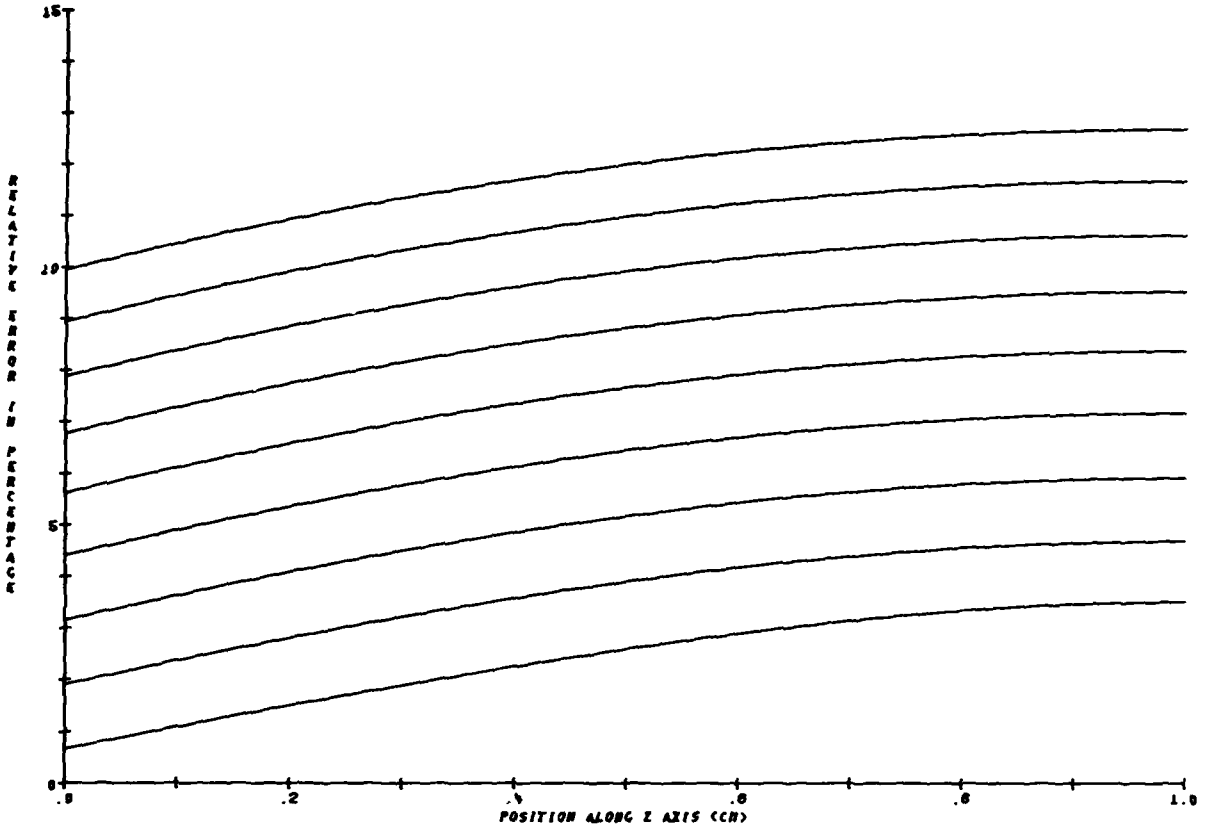

FIGURE 5 - Percentage of error in temperature distribution between the two models of Fig. 3.

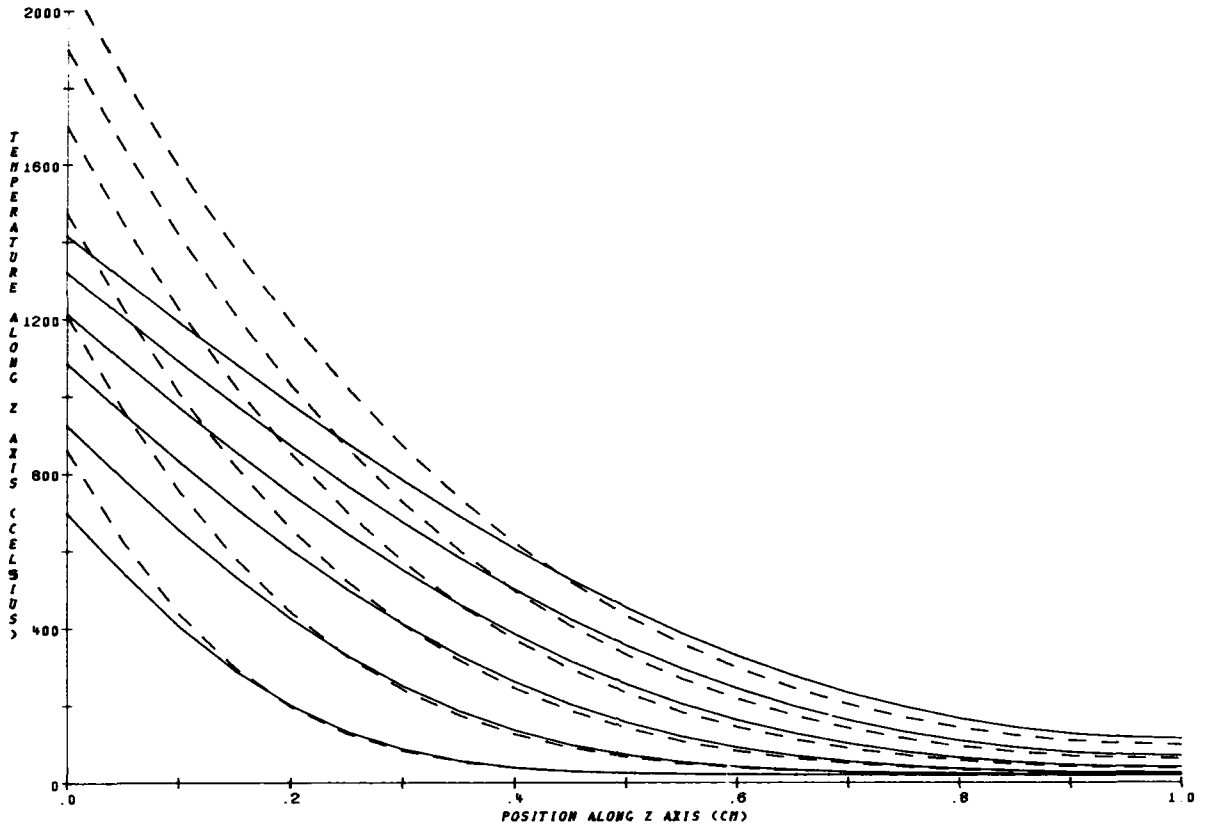

FIGURE 6 - Temperature distribution within a 1 cm-thick stainless steel #304 target (21 nodes along z axis) for an incident intensity of 20,000 W/cm^2 and a coupling coefficient of 0.04. The time interval between each curve is 0.25 s for the temperature-dependent case (continous lines) and for the constant room-temperature case (alternating lines).

Furthermore, the curves cross one another and we find a higher value of the temperature on the back surface in the variable case. Figure 7 shows the absolute error in temperature along the z axis for the same time interval.

4.2.3 Averaging of the Thermophysical Properties

We define the average value of the thermophysical properties in the following way:

$$K_{av.} = \frac{K(T_i) + K(T_m)}{2} \qquad [30]$$

and

$$C_{pav.} = \frac{C_p(T_i) + C_p(T)_m}{2} \qquad [31]$$

where T_i is the initial temperature and T_m the melting temperature. If we use these values in the constant properties model instead of those of the room temperature, we obtain the results shown in Fig. 8 for copper and those in Fig. 9 for stainless steel #304. We expect similar results because the thermophysical properties of these two materials vary linearly with temperature so that these properties are overestimated at low temperature and underestimated at high temperature by the average properties values. However, although the discrepancy in time to reach melting on the front surface is removed, the temperature distribution through the slab, specially in stainless steel #304 is quite different. The distribution behaves as if the coupling coefficient was varying with temperature and, depending on the position selected along the z axis, it seems to increase or to decrease with time.

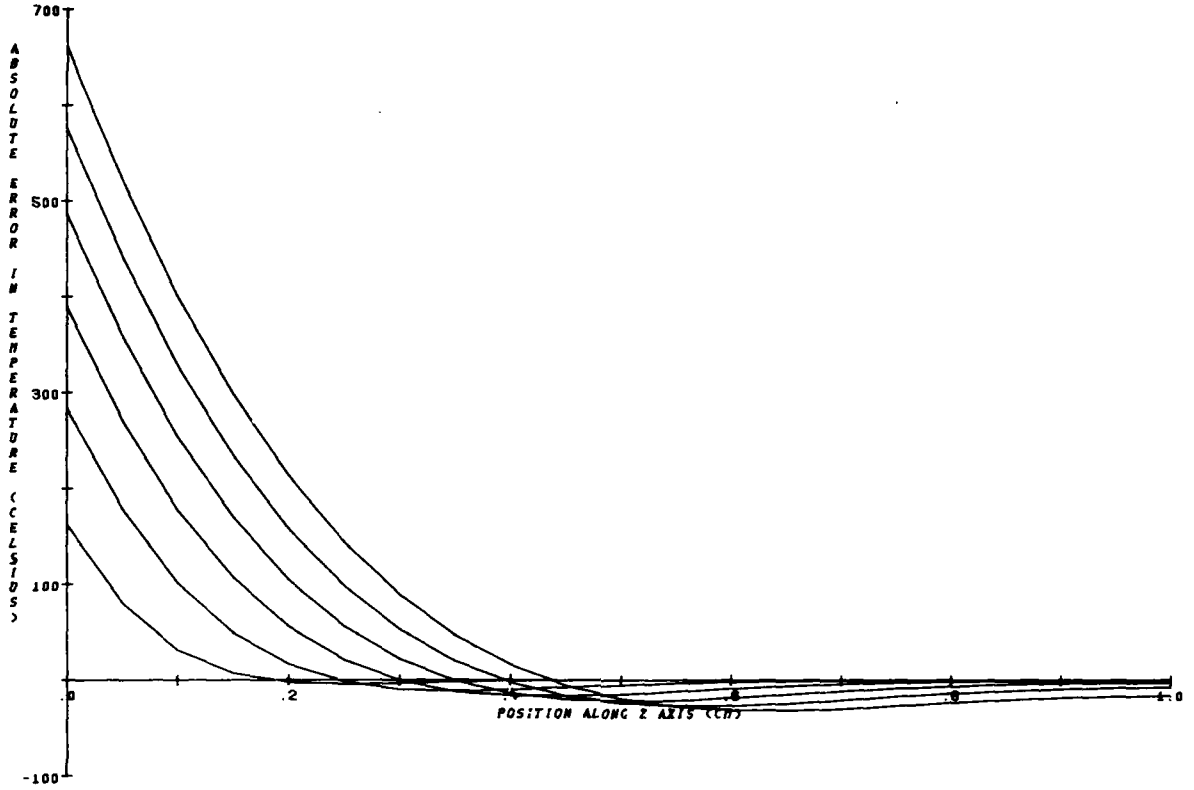

FIGURE 7 - Absolute error in temperature distribution for conditions of Fig. 6.

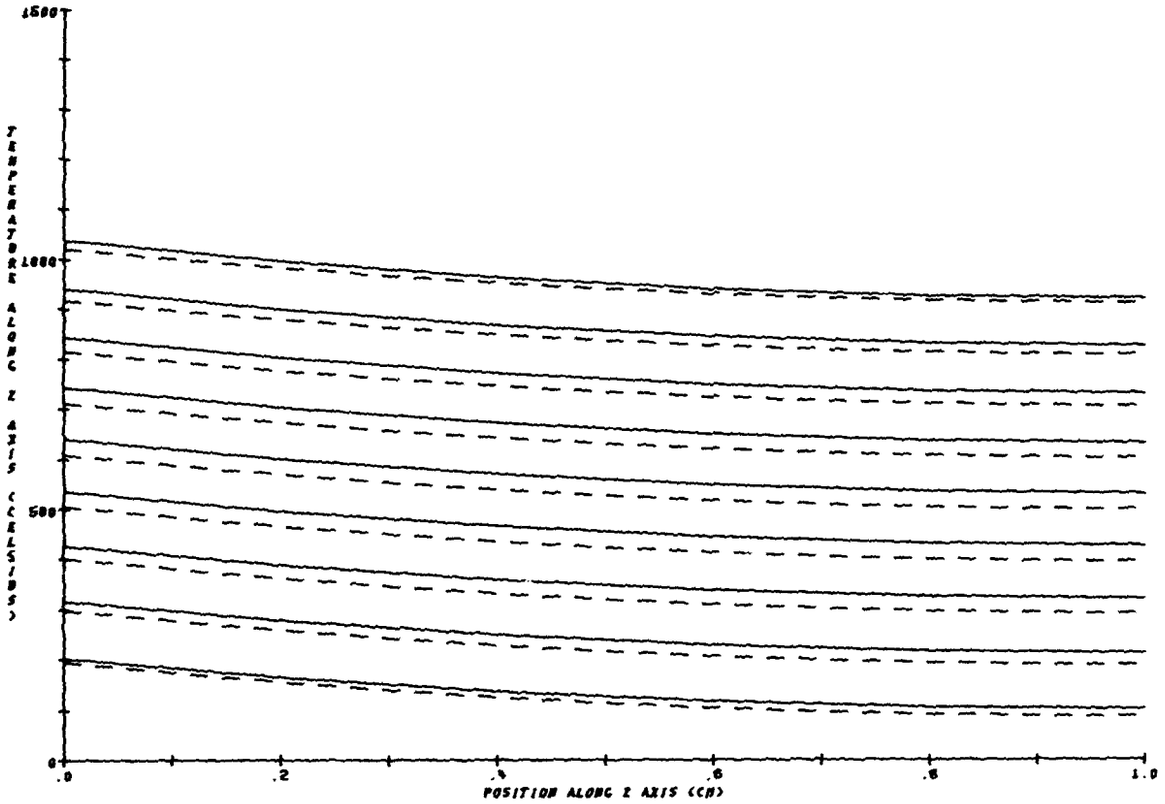

FIGURE 8 - Temperature distribution within a 1 cm-thick Cu target (6 nodes along z axis) for an incident intensity of 20,000 W/cm^2 and a coupling coefficient of 0.04. The time interval between each curve is 0.25 s for the temperature-dependent case (continuous lines) and the average-value case (alternating lines).

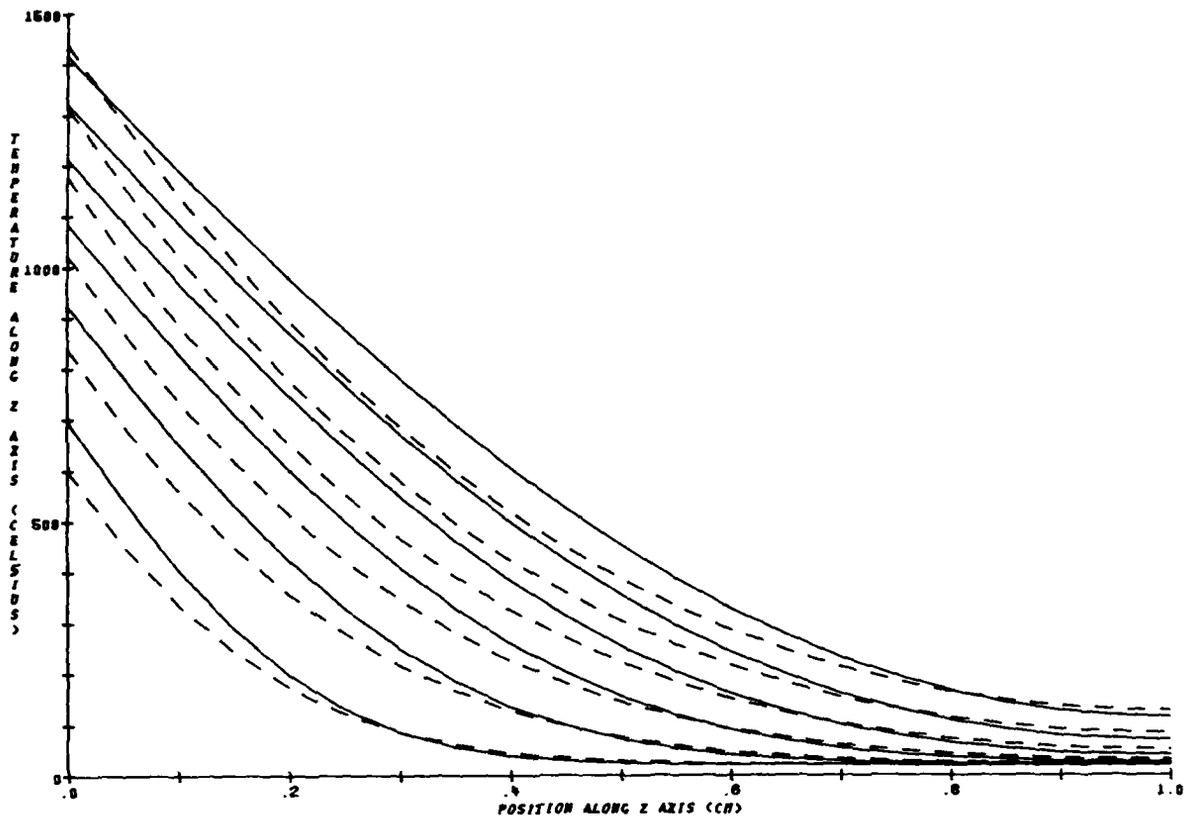

FIGURE 9 - Temperature distribution within a 1 cm-thick stainless steel #304 target (21 nodes along z axis) for an incident intensity of 20,000 W/cm^2 and a coupling coefficient of 0.04. The time interval between each curve is 0.25 s for the temperature-dependent case (continuous lines) and the average-value case (alternating lines).

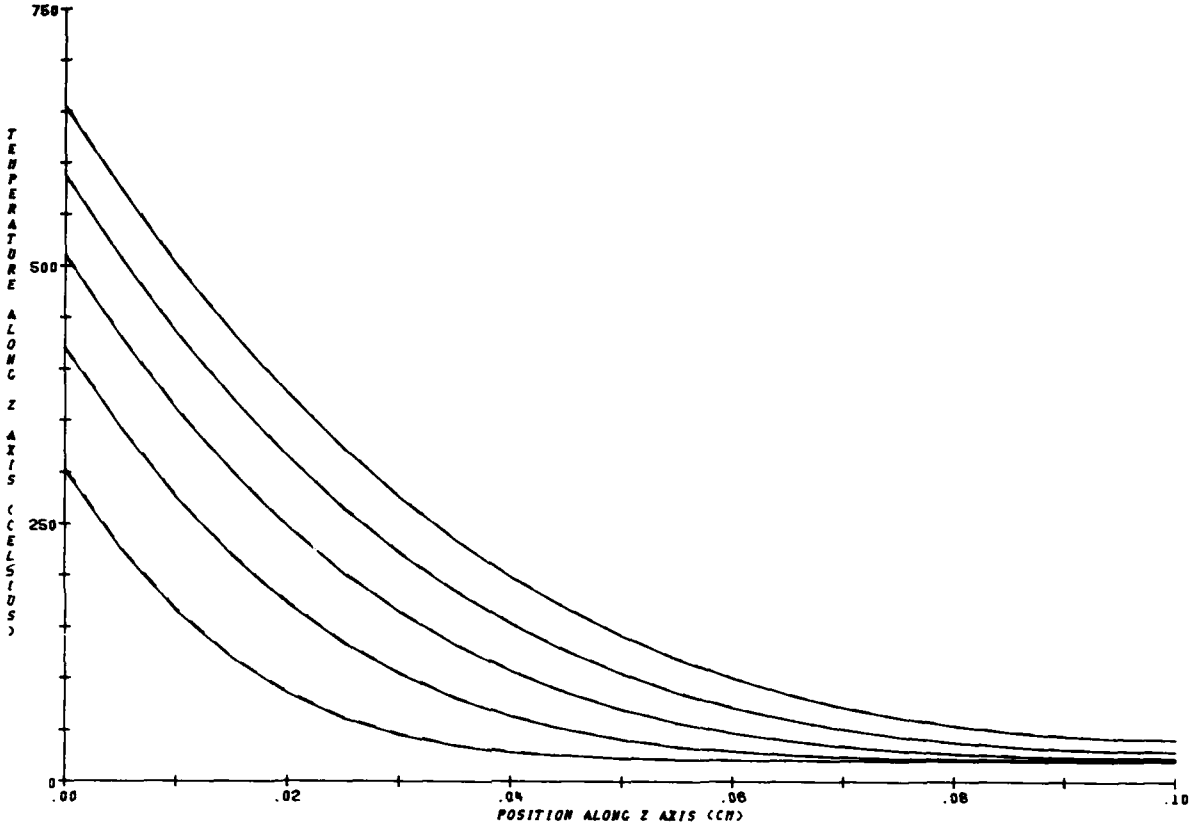

FIGURE 10 - Temperature distribution within a 0.1 cm-thick Al target (21 nodes along z axis) for an incident intensity of 2×10^{6} W/cm^2 and a coupling coefficient of 0.02. The time interval between each curve is 134×10^{-6} s for the numerical case (continuous lines) and the analytical average value case (alternating lines).

Finally, Fig. 10 presents some results for aluminum, using the average properties values as defined previously. We used 21 nodes for this 0.1 cm-thick slab because we were interested in a high-input intensity ($\phi = 2 \times 10^6$ W/cm^2) for a short time duration, as would be encountered with pulsed lasers. The time to reach melting on the front surface is within 1% of the one obtained by Gautier (Ref. 12).

5.0 DISCUSSION

Our aim of developing a reliable numerical procedure for the non-linear one-dimensional heat conduction equation has been achieved. The boundary conditions are calculated through a numerical procedure different from the one used by Hanley (Ref. 1); therefore, we satisfy the energy conservation law whereas his scheme does not. Furthermore, our scheme is simpler, easier to understand and to work with, and through proper selection of the "stability constant", converges more rapidly to the true solution for an optimal number of steps. The time-independent or continuous-intensity laser beam has been considered in the present work.

Our present solution is applicable to cases where lateral conduction of heat is negligible. These situations correspond to short interaction time consideration or to experiments in which the laser beam dimensions are similar or larger than those of the target. However, extension of our numerical model to 3 dimensions is easy and straightforward.

Similarly, the model does not include any explicit terms for radiative and convective heat losses but these could be considered by modifying the appropriate boundary conditions.

6.0 CONCLUSIONS

A numerical method of solving the nonlinear partial differential equations of heat conduction with a computer has been developed. The reliability of the numerical results has been demonstrated by comparison with the analytical solution in one dimension. By proper selection of the "stability constant" the numerical procedure converges more rapidly to the results of the analytical solution by minimizing the truncation error. Agreement is within 1% after only 25 time steps (25 Δt).

We have shown the importance of taking into account the effect of temperature-dependent thermophysical properties when dealing with laser-matter interactions. For example, in the case of stainless steel #304, the calculated time required to reach melting on the front surface in the case of variable properties is twice the time necessary when room-temperature values are used. Although this discrepancy disappears when average-temperature values are used, the calculated temperature distributions through the material are significantly different.

7.0 ACKNOWLEDGMENTS

The author wishes to thank Drs. M. Gravel and R.W. MacPherson for their valuable suggestions and discussions. He also recognizes the valuable participation of Mr. J.C. Anctil in the preliminary stage of posing the problem. The full collaboration of Mr. A. Blanchard, R. Gouge and R. Tremblay from Data Systems was a great asset in the use of the computer.

8.0 REFERENCES

1. Hanley, S.T., "Heat Conduction in Three Dimensions", NRL Report 8066, December 1976.

2. Carslaw, H.S., and Jaeger, J.C., "Conduction of Heat in Solids", 2nd ed., Oxford University Press, Oxford 1959.

3. Ozisik, M.N., "Boundary Value Problems of Heat Conduction", International Textbook Co., Scranton, Pens., 1968.

4. Ames, W.F., "Nonlinear Partial Differential Equations in Engineering" Academic Press, New York, 1965.

5. Cobble, H.H., "Nonlinear Heat Transfer in Solids", Technical Report No. 8, January 1963. Mechanical Engineering Department, Eng. Expt. Station, New Mexico State University, University Park, N.M.

6. Fox, L., "Numerical Solution of Ordinary and Partial Differential Equations", Addison-Wesley Publishing Company Inc., Reading, Mass. 1962.

7. Smith, G.D., "Numerical Solution of Partial Differential Equations with Exercises and Worked Solutions", Oxford University Press, London 1965.

8. Richtmeyer, R.D., "Difference Methods for Initial Value Problems", Interscience Publishers, Inc., New York, 1957.

9. Price, P.H. and Slack, M.R., "Stability and Accuracy of Numerical Solutions of the Heat Flow Equation", Br. J. Appl. Ph. Vol. 3, pp. 379-384, December 1952.

10. Schriempf, J.T., "Response of Materials to Laser Radiation: A Short Course", NRL Report 7728, July 1974.

11. Touloukian, Y.S., Powell, R.W., Ho, C.Y., Nicolaou, M.C., "Thermophysical Properties of Matter", IFI/Plenum, N.Y., 1973, Vol. 10, p. 51.

12. Gautier, B., "Conduction de la chaleur dans un solide en ablation sous l'action d'un rayonnement laser intense", Rapport R 122/76 Institut Saint-Louis, France, Juin 1976.

APPENDIX A

A.1 Program Description and Listing

The program written in Fortran IV may be used under the CP-V Version E01 operating system on DREV Xerox 560 MP computer. The listing shows the materials, with their corresponding thermophysical properties, available to the user. Having selected the material, the user inputs the thickness of his target, the number of nodes through it, the ambient temperature, the incident flux, its angle of incidence from normal, the coupling coefficient, the total time of run, the print out interval and the type of boundary conditions. From there on, the program starts its calculation by establishing the initial conditions throughout the slab. Then, it determines the temperature for the next time increment and checks if it has to print out those results. In the event it has, we obtain tables of values for the front and back surface temperature and its distribution through the slab. Furthermore, it calculates, for this time, the corresponding analytical solution and outputs it. Then, the program checks if the total run time is exhausted and if not, it goes back through the loop and calculates the temperature distribution for the next time step. Once the alloted time is passed the program calls subroutines to create APL files with the complete set of data. These files are used to produce graphical representations similar to the ones appearing in this report.

```
1.000 °JOB 66043,JPBMORENCY,7. (TERMINAL JOB BFALACOCA).
2.000 °LIMIT (TIME,20),(CORE,48)
3.000 °ASSIGN F:105,(FILE,HTINPUT1),(IN)
5.500 °ASSIGN M:SI,(FILE,FALACOCA1),(IN)
6.000 °FORTRAN LS,SI,GO,BC
7.000 °LOAD (GO),(LMN,FALACOCALM),(PERM),(EF,(APLFNS,LPR))
8.000 °RUN
*
```

ONE-DIMENSION HEAT CONDUCTION LISTING

```
      DIMENSION U0(0:21,2),T0(21,2),T3RA(21,150),T0(21),TM(21,100)
      DOUBLE PRECISION F8
    1 FORMAT('1')
   10 FORMAT(' 1 ...ALUMINUM, 2 ...COPPER, 3 ...MOLYBDENUM,')
   20 FORMAT(' 4 ...IRON, 5 ...NICKEL, 6 ...TITANIUM, 7 ...AL(2024)')
   25 FORMAT(' 8 ...STAINLESS STEEL(304)')
   30 FORMAT(' INPUT # FOR TARGET MATERIAL')
   40 FORMAT(I4)
   50 FORMAT(' MATERIAL THICKNESS (CM)')
   51 FORMAT('NUMBER OF NODES ALONG Z-AXIS')
   55 FORMAT(2I5,F20.5)
   60 FORMAT(F20.5)
   90 FORMAT(' AMBIENT TEMPERATURE (C)')
  100 FORMAT(' INCIDENT INTENSITY (WATTS/CM*CM) ')
  120 FORMAT(' ANGLE OF INCIDENCE (DEG) FROM NORMAL')
  123 FORMAT(' PREMELT ABSORPTION COEFFICIENT')
  130 FORMAT(' TIME OF RUN (SEC)')
  135 FORMAT(' PRINT OUT INTERVAL (SEC)')
  150 FORMAT(' 1 ...BACK SURFACE INSULATED ')
  160 FORMAT(' 2 ...BACK SURFACE HEAT SINKED TO AMBIENT ')
  185 FORMAT('FRONT SURFACE STARTS TO MELT AT POSITION (1)
     1AND AT TIME T=  ',F10.5,'   SECONDS')
  190 FORMAT('1TIME IN SECONDS',F11.7,///)
  191 FORMAT('0FRONT SURFACE')
  192 FORMAT(6F15.8)
  193 FORMAT('0BACK SURFACE')
  194 FORMAT('0TEMPERATURE ALONG Z-AXIS')
  195 FORMAT(' RUN COMPLETED')
  196 FORMAT('0ANALYTICAL SOLUTION ALONG Z-AXIS')
      WRITE (108,1)
C      SELECT..... MATERIAL CODE
      WRITE (108,10)
      WRITE (108,20)
      WRITE (108,25)
      WRITE (108,30)
      READ (105,40) I11
      OUTPUT I11
      GO TO (200,210,220,230,240,241,242,245),I11
  200 CONTINUE
C     I11=1 ...ALUMINUM
      A0=660.
      F0=.25
      F2=.57361
      A3=2.7
```

```
      A4=94.
      F1=0.
      F3=0.
      F4=0.
      F5=30.
      F9=2.43
      GO TO 300
  210 CONTINUE
C     I11=2 ...COPPER
      A0=1083.
      F0=.091
      F2=.956
      A3=8.89
      A4=42.
      F1=2.456E-5
      F3=1.567E-4
      F4=0.
      F5=0.0
      F9=8.217
      GO TO 300
  220 CONTINUE
C     I11=3 ...MOLYBDENUM
      A0=2610.
      F0=.06162
      F2=.3460
      A3=10.2
      A4=131.
      F1=2.2E-5
      F3=3.46E-5
      F4=0.
      F5=10.
      F9=8.1
      GO TO 300
  230 CONTINUE
C     I11=4 ...IRON
      A0=1535.
      F0=.1060
      F2=.1080
      A3=7.85
      A4=65.
      F1=9.6E-5
      F3=1.08E-5
      F4=0.
      F5=18.
```

```
      F9=6.88
      GO TO 300
  240 CONTINUE
C     I11=5 ...NICKEL
      A0=1453.
      F0=.1095
      F2=.1425
      A3=8.75
      A4=73.
      F1=5.49E-5
      F3=-4.56E-5
      F4=0.
      F5=0.
      F9=7.9
      GO TO 300
  241 CONTINUE
C     I11=6 ...TITANIUM
      A0=1690.
      F0=.139
      F2=.0372
      A3=4.54
      A4=103.9
      F1=0.
      F3=-4.E-6
      F4=0.
      F5=21.
      F9=4.09
      GO TO 300
  242 CONTINUE
C     I11=7 ...AL(2024)
      A0=630.
      F0=.215
      F2=.334
      A3=2.77
      A4=95.6
      F1=7.7E-5
      F3=9.0E-4
      F4=0.
      F5=0.
      F9=2.43
      GO TO 300
  245 CONTINUE
C     I11=8 ...ACIER(304)
      A0=1450.
```

```
      F0=.11712
      F2=.03615
      A3=7.9
      A4=65.
      F1=3.74E-5
      F3=3.32E-5
      F4=0.
      F5=20.
      F9=7.
  300 CONTINUE
C      INPUT..... MATERIAL THICKNESS (CM)
      WRITE (108,50)
      READ (105,60) A6
      OUTPUT A6
C      INPUT.....NUMBER OF NODES ALONG Z-AXIS
      WRITE(108,51)
      READ(105,60) KK
      OUTPUT KK
      NK=KK-1
C      INPUT..... AMBIENT TEMPERATURE (C)
      WRITE (108,90)
      READ (105,60) A9
      OUTPUT A9
C      INPUT..... INCIDENT INTENSITY (WATTS/CM*CM)
      WRITE (108,100)
      READ (105,60) B0
      OUTPUT B0
      B0=B0/4.184
C      INPUT..... ANGLE OF INCIDENCE (DEG) FROM NORMAL
      WRITE (108,120)
      READ (105,60) B2
      OUTPUT B2
C      INPUT..... PREMELT ABSORPTION COEFFICIENT
      WRITE (108,123)
      READ (105,60) A5
      OUTPUT A5
C      INPUT..... TIME OF RUN (SEC)
      WRITE (108,130)
      READ (105,60) B3
      OUTPUT B3
C      INPUT..... PRINT OUT INTERVAL (SEC)
      WRITE (108,135)
      READ (105,60) D0
      OUTPUT D0
```

```
      C9=0.
C      SELECT.....BOUNDARY CONDITIONS: IB5
      WRITE (108,150)
      WRITE (108,160)
C.....IB5=1 .) BACK SURFACE INSULATED
C.....IB5=2 .) BACK SURFACE HEAT-SINKED TO AMBIENT
      READ (105,40) IB5
      OUTPUT IB5
C      FRONT SURFACE.....INCIDENT FLUX
      P=B0
      D1=D0
      INDI=0.
C      INITIAL CONDITIONS
      DO 344 K=1,KK
      T0(K,1)=A9
      IF(F3.EQ.0.) GO TO 345
      U0(K,1)=A9-F5-F3*F5*A9/F2+.5*F3*F5*F5/F2+.5*F3*A9*A9/F2
      GO TO 344
345   U0(K,1)=A9
344   CONTINUE
      CTE=1./6.
      C2=CTE*(F0+F1*A9)*A3*A6*A6/(F2+F3*(A9-F5))/NK/NK
      C0=C2*NK*NK/A6/A6
      C4=2.*C2*NK*NK/A6/A6
      THET=3.141592*B2/180.
      G3=COS(THET)*A5*A6*2./NK
500   IF(T0(1,1).LE.A0)      GO TO 505
      WRITE(108,185),C9
      GO TO 1000
505   CONTINUE
      F8=A3
      DO 560 K=1,KK
      U0(0,1)=U0(2,1)+G3*P/F2
      GO TO (530,535),IB5
530   U0(KK+1,1)=U0(KK-1,1)
      GO TO 550
535   U0(KK+1,1)=2.*U0(KK,1)-U0(KK-1,1)
550   CONTINUE
      A1=(F2+F3*(T0(K,1)-F5))/F8/(F0+F1*T0(K,1))
      E1=A1*C0*(U0(K+1,1)+U0(K-1,1))
      U0(K,2)=E1+(1.-A1*C4)*U0(K,1)
      IF(F3.EQ.0.0) GO TO 555
      BETA=F3/F2
      T0(K,2)=((((1.+2.*BETA*U0(K,2))**.5)/BETA)+F5-1./BETA)
```

```
221.            GO TO 560
222.      555   TO(K,2)=UO(K,2)
223.      560   CONTINUE
224.            C9=C9+C2
225.      580   IF(C9.LT.D1) GO TO 900
226.            D1=D1+DO
227.            INDI=INDI+1
228.            DO 600 K=1,KK
229.            TGRA(K,INDI)=TO(K,1)
230.      600   CONTINUE
231.            TDIM=C9-C2
232.            WRITE(108,190) TDIM
233.            WRITE(108,191)
234.            WRITE(108,192) (TO(1,1))
235.            WRITE(108,193)
236.            WRITE(108,192) (TO(KK,1))
237.            WRITE(108,194)
238.            WRITE(108,192) (TO(L,1),L=1,KK)
239.      C.....ANALYTICAL SOLUTION
240.            LL=INDI
241.            PI=3.14159265
242.            DIFF=(F2+F3*(AO-F5)/2.)/A3/(FO+F1*(AO-F5)/2.)
243.      700   Z=0.0
244.            J=1
245.      725   W1=EXP(-DIFF*PI*PI*TDIM/A6/A6)
246.            N=1
247.            C=0.0
248.      750   W=(-1)**N/N/N*EXP(-DIFF*N*N*PI*PI*TDIM/A6/A6)
249.            W2=W*COS(N*PI*(A6-Z)/A6)
250.            VI=ABS(W/W1)
251.            IF(VI.LE.0.000002) GO TO 775
252.            C=C+W2
253.            N=N+1
254.            GO TO 750
255.      775   C=C+W2
256.            TO(J)=A5*P*TDIM*DIFF/(F2+F3*(AO-F5)/2.)/A6+A5*P*A6/(F2+F3*(
257.           1AO-F5)/2.)*((3*(A6-Z)**2-A6*A6)/6./A6/A6-2.*C/PI/PI)+A9
258.            Z=Z+A6/20.
259.            J=J+1
260.            IF(Z.GT.A6) GO TO 800
261.            GO TO 725
262.      800   WRITE(108,196)
263.            WRITE(108,192) (TO(J),J=1,21)
264.            DO 850 I=1,21
```

```
      TM(I,LL)=TO(I)
  850 CONTINUE
C.....END OF ANALYTICAL SOLUTION
  900 IF(C9.GT.B3.OR.C9.EQ.B3) GO TO 950
      DO 910 K=1,KK
      UO(K,1)=UO(K,2)
      TO(K,1)=TO(K,2)
  910 CONTINUE
      GO TO 500
  950 WRITE(108,195)
 1000 CONTINUE
      CALL GRAPH(TM,INDI,21,1)
      CALL GRAPH(TGRA,INDI,KK,5)
      CALL EXIT
      END
```

```
      SUBROUTINE GRAPH(TEMP,INDI,KK,IAN)
      DIMENSION TEMP(KK,INDI)
      DIMENSION ITYPE(2),ISIZE(3)
      ISIZE(1)=2
      ISIZE(2)=21
      ISIZE(3)=INDI
      ITYPE(1)=3
      ITYPE(2)=4
      CALL FTIE(1,'JCAOUT')
      CALL FREPLACE(1,IAN,TEMP,ISIZE,ITYPE)
      ITYPE(1)=2
      ITYPE(2)=2
      ISIZE(1)=0
      CALL FREPLACE(1,100,KK,ISIZE,ITYPE)
      CALL FREPLACE(1,101,INDI,ISIZE,ITYPE)
      CALL FUNTIE(1)
      RETURN
      END
```

A.2 Input and Output Examples

The program is run from a terminal in two possible modes. In the ON-LINE interactive mode the program asks for the specific input file considered and then starts the calculation. The output is displayed on the terminal used and is similar to that obtained in the BATCH mode. In the BATCH mode, a job file, which contains a set of controls, the program and data input and output files, are run. The output is printed on the computer line printer as shown in the typical example shown hereafter.

INPUT DATA FILE

```
 1 ...ALUMINUM, 2 ...COPPER, 3 ...MOLYBDENUM,
 4 ...IRON, 5 ...NICKEL, 6 ...TITANIUM, 7 ...AL(2024)
 8 ...STAINLESS STEEL(304)
 INPUT # FOR TARGET MATERIAL
 I11 = 8
 MATERIAL THICKNESS (CM)
 A6 = 1.00000
NUMBER OF NODES ALONG Z-AXIS
 KK = 21
 AMBIENT TEMPERATURE (C)
 A9 = 20.0000
 INCIDENT INTENSITY (WATTS/CM*CM)
 B0 = 20000.0
 ANGLE OF INCIDENCE (DEG) FROM NORMAL
 B2 = .000000
 PREMELT ABSORPTION COEFFICIENT
 A5 = 4.000000E-02
 TIME OF RUN (SEC)
 B3 = 3.00000
 PRINT OUT INTERVAL (SEC)
 D0 = .250000
 1 ...BACK SURFACE INSULATED
 2 ...BACK SURFACE HEAT SINKED TO AMBIENT
 IB5 = 1
```

OUTPUT DATA FILE

TIME IN SECONDS .2468463

FRONT SURFACE
517.17797852

BACK SURFACE
20.00000000

TEMPERATURE ALONG Z-AXIS

517.17797852	349.60815430	217.49487305	125.55175781	70.09808594	41.05175781
27.87646484	22.62304688	20.77685547	20.20263672	20.04687500	20.00952148
20.00122070	20.00000000	20.00000000	20.00000000	20.00000000	20.00000000
20.00000000	20.00000000	20.00000000			

ANALYTICAL SOLUTION ALONG Z-AXIS

430.88012695	290.82983398	188.14064026	117.88738257	73.20011902	46.90753174
32.62438965	25.48023987	22.19616699	20.81092834	20.27543640	20.08557129
20.02426147	20.00599670	20.00085449	19.99990845	19.99990845	19.99990845
19.99971008	19.99990845	20.00009155			

TIME IN SECONDS .4936965

FRONT SURFACE
693.62304688

BACK SURFACE
20.00000000

TEMPERATURE ALONG Z-AXIS

693.62304688	537.38012695	399.22753906	283.46118164	196.53442383	126.16528320
81.33715820	53.30810547	37.02905273	28.20971680	23.73413086	21.60327148
20.64916992	20.24731445	20.08837891	20.02905273	20.00952148	20.00219727
20.00000000	20.00000000	20.00000000			

ANALYTICAL SOLUTION ALONG Z-AXIS

601.07006836	455.33862305	336.76147461	243.46356201	172.60578918	120.73976135
84.19859314	59.44902039	43.34881592	33.29827881	27.26207397	23.83041382
21.93449402	20.93702698	20.43501282	20.19314575	20.08219910	20.03311157
20.01274109	20.00474548	20.00303650			

TIME IN SECONDS .7405447

FRONT SURFACE
820.00000000

BACK SURFACE
20.01562500

TEMPERATURE ALONG Z-AXIS

820.00000000	672.2712e023	536.358398e4	415.2e316406	311.39135742	226.2580566e
159.8e691602	110.84252930	76.50537109	53.70288086	39.30004883	30.62207031
25.62304688	22.86e01367	21.40307617	20.66162109	20.29907227	20.13085938
20.05517578	20.02e90234	20.01562500			

ANALYTICAL SOLUTION ALONG Z-AXIS

731.66186523	583.39e04297	457.50317383	352.9443359e	268.0e398438	200.84373474
149.86979675	109.70841980	80.96261597	60.41841125	46.13006592	36.46318054
30.10462952	26.03887939	23.51322937	21.989e8669	21.0977e780	20.59326172
20.32151794	20.19039917	20.15176392			

TIME IN SECONDS .9981252

FRONT SURFACE
925.62231445

BACK SURFACE
20.25854492

TEMPERATURE ALONG Z-AXIS

925.62231445	784.7021e844	652.32104492	530.60986328	421.55859375	326.76611328
247.17163086	182.84936523	132.94091797	95.79077148	69.24682617	51.01342773
38.94702148	31.23779297	26.47460938	23.62622070	21.97729492	21.05395508
20.56298828	20.32714844	20.25854492			

ANALYTICAL SOLUTION ALONG Z-AXIS

848.21044922	696.37353516	565.90307617	454.12353516	359.96093750	282.01391602
218.64e68547	168.07295227	128.47384644	98.06254578	75.16455078	58.26657104
45.04951477	37.39862061	31.40240479	27.33912659	24.65455627	22.93768311
21.89921570	21.34771729	21.17568970			

TIME IN SECONDS 1.2449541

FRONT SURFACE
1011.34643555

BACK SURFACE
21.30419922

TEMPERATURE ALONG Z-AXIS

1011.34643555	875.65283203	746.64135742	625.93310547	515.12182617	415.64184570
328.59887695	254.60668945	193.66650391	145.12255859	107.74902344	79.93212891
59.89379883	45.90429688	36.42260742	30.17968750	26.18798828	23.72265625
22.27929688	21.53271484	21.30419922			

ANALYTICAL SOLUTION ALONG Z-AXIS

942.73046875	791.87182617	658.401855547	541.83129883	441.37695313	356.00170898
284.47045898	225.44110107	177.37393188	138.89701843	108.55567932	85.00825500
67.03033447	53.53417969	43.58168030	36.38682556	31.31039429	27.85150146
25.65603210	24.40707397	24.01371765			

TIME IN SECONDS 1.4917831

FRONT SURFACE
1086.60424805

BACK SURFACE
24.01245117

TEMPERATURE ALONG Z-AXIS

1086.60424805	955.26074219	829.37280273	710.21801758	599.09204102	497.22680664
405.69165039	325.27392578	256.37207031	198.91552734	152.35009766	115.69091797
87.65380859	66.80859375	51.73193359	41.12133789	33.86914063	29.09033203
26.12451172	24.51928711	24.01245117			

ANALYTICAL SOLUTION ALONG Z-AXIS

1030.06884766	878.45361328	742.752441 41	622.59082031	517.36499023	426.26879883
348.32910156	282.44848633	227.44612122	182.10473633	145.20967102	115.58514404
92.12615967	73.81950378	59.76214600	49.16986084	41.38488770	35.87284851
32.22424316	30.14958191	29.47726440			

TIME IN SECONDS 1.7493439

FRONT SURFACE
1156.86865234

BACK SURFACE
29.54296875

TEMPERATURE ALONG Z-AXIS

1156.86865234	1029.38769531	906.46044922	789.12060547	678.42895508	575.43090820
481.09497070	396.23071289	321.40991211	256.88818359	202.55200195	157.91894531
122.17993164	94.28608894	73.07543945	57.36938477	46.08593750	38.29370117
33.25634766	30.44555664	29.54296875			

ANALYTICAL SOLUTION ALONG Z-AXIS

1113.79589844	961.56835937	824.05737305	700.96704102	591.81860352	495.96777344
412.63110352	340.91357422	279.84057617	228.39111328	185.52926636	150.23272705
121.52125549	98.47674084	80.26164246	66.13415527	55.45605469	47.70117188
42.45678711	39.42846680	38.43872070			

TIME IN SECONDS 1.9961729

FRONT SURFACE
1218.06225586

BACK SURFACE
38.14111328

TEMPERATURE ALONG Z-AXIS

1218.06225586	1093.79028320	973.43701172	857.86254883	747.98118164	644.62866211
548.73120117	461.04028320	382.17993164	312.55859375	252.32128906	201.31542969
155.09350586	124.95654297	98.02758789	77.34228516	61.94262695	50.95410156
43.65087891	39.49096680	38.14111328			

ANALYTICAL SOLUTION ALONG Z-AXIS

1188.42285156	1035.72387695	896.81689453	771.45874023	659.25537109	559.67358398
472.06201172	395.66967773	329.67211914	273.19702148	225.34904480	185.23338318
151.98117065	124.76715088	102.82881165	85.48120117	72.12719727	62.26831055
55.51147461	51.57177734	50.27758789			

TIME IN SECONDS 2.2430019

FRONT SURFACE
1274.430419?2

BACK SURFACE
50.40991211

TEMPERATURE ALONG Z-AXIS

1274.430419?2	1152.99023438	1034.98266602	921.13524391	812.21191406	708.99047852
612.23535156	522.66796875	440.90844727	367.44189453	302.55639648	246.32324219
198.56884766	158.88574219	126.67724609	101.22167969	81.744140?3	67.49609375
57.82836914	52.23754883	50.40991211			

ANALYTICAL SOLUTION ALONG Z-AXIS

1258.57446289	1105.48559570	965.42089844	838.17749023	723.42456055	620.71313477
529.49145508	449.12158203	378.89770508	318.06787109	268.50400391	227.47293091
184.15600586	153.16?5872?	127.82128906	107.49462891	91.6?184570	79.80322266
71.61254883	66.80566406	65.22119141			

TIME IN SECONDS 2.4898310

FRONT SURFACE
1326.81542969

BACK SURFACE
66.54907227

TEMPERATURE ALONG Z-AXIS

1326.81542969	1207.90551758	1092.04345703	979.85742188	872.00585937	769.17065430
672.03344727	581.25219727	497.42944336	421.07373047	356.56225586	292.10693359
239.73242188	195.26977539	158.36865234	128.54541016	105.23315430	87.84887695
75.86474609	68.85424805	66.54907227			

ANALYTICAL SOLUTION ALONG Z-AXIS

1324.98828125	1171.57031250	1030.52929688	901.69262695	784.77856445	679.40356445
585.09643555	501.30810547	427.43017578	362.81005859	306.76953125	258.62133789
217.68812561	183.31578064	154.89184570	131.85742188	113.71899414	100.05981445
90.54614258	84.93652344	83.08276367			

```
TIME IN SECONDS  2.7+73917


FRONT SURFACE
 1377.909+2383

BACK SURFACE
   87.51660156

TEMPERATURE ALONG Z-AXIS
 1377.909+2383  1261.380e5938  1147.57592773  1037.04199219   93[.3832718   82[.110107+2
  736.91772+61   639.37939+53   [54.063+7656   +75.+82+2188   +[+.[6250000  3+0.11+99023
  283.81103516   235.16967773   194.06103516   160.22531836   133.31372070  112.93090820
   96.69506836    80.293+5703    87.51660156

ANALYTICAL SOLUTION ALONG Z-AXIS
 1396.91577+8  1237.20581055  1095.29736328   965.0+2+A0+7   6+[.20117188  739.+[+5312[[
  6+1.37011719   55+.50[9[625   +77.32128906   +09.25781250   3+[.7233[867  299.11[+0820
  253.d+[78540   216.33911133   185.0+7607+2   159.+7879977   135.19287109  123.81689+[3
  113.0[249023   106.58237305   10+.57397+61


TIME IN SECONDS  2.99+2207


FRONT SURFACE
 1+23.96826172

BACK SURFACE
   111.+05273++

TEMPERATURE ALONG Z-AXIS
 1+23.96826172  1309.50903320  1197.52+65820  1088.+9[33789   98[.93530273   881.376+6+8+
  7[+.36791992   692.+[39375[   [06.19+[2+22   526.07397+61   +[[.[[[0+883   385.99+1+063
  3[[.67675781   27+.75[[773+   230.28198242   193.1711+258   16[.2[68+570   1+0.35009766
  12+.19238281   11+.59[08789   111.+05273++

ANALYTICAL SOLUTION ALONG Z-AXIS
 1+51.33032227  1297.37[[6281  1154.75659180  1023.33328[95   90[.[[087891   793.17602535
  69[.8[[39[+8   60+.38276008   52+.++506836   +53.50170898   3[1.[3[88867   336.52001953
  2[[.+[139648   2+9.26220703   215.53198242   187.[007[125   16[.[7797852   1+[.8305664+1
  13[.99218750   129.96826172   127.64013672
RUN COMPLETED
+EXIT+
```

DREV R-4166/80 (UNCLASSIFIED)

Research and Development Branch, DND, Canada.
DREV, P.O. Box 880, Courcelette, Que. G0A 1R0

"A One-Dimensional Numerical Model of Laser Heating of Target Slabs"
by J.P. Morency

This report establishes a numerical scheme to solve the nonlinear one-dimensional heat transfer equation. The scheme is then applied to the case of laser-metals interaction and used to show the importance of thermo-physical properties variation on the temperature distribution within a slab. (U)

DREV R-4166/80 (UNCLASSIFIED)

Research and Development Branch, DND, Canada.
DREV, P.O. Box 880, Courcelette, Que. G0A 1R0

"A One-Dimensional Numerical Model of Laser Heating of Target Slabs"
by J.P. Morency

This report establishes a numerical scheme to solve the nonlinear one-dimensional heat transfer equation. The scheme is then applied to the case of laser-metals interaction and used to show the importance of thermo-physical properties variation on the temperature distribution within a slab. (U)

DREV R-4166/80 (UNCLASSIFIED)

Research and Development Branch, DND, Canada.
DREV, P.O. Box 880, Courcelette, Que. G0A 1R0

"A One-Dimensional Numerical Model of Laser Heating of Target Slabs"
by J.P. Morency

This report establishes a numerical scheme to solve the nonlinear one-dimensional heat transfer equation. The scheme is then applied to the case of laser-metals interaction and used to show the importance of thermo-physical properties variation on the temperature distribution within a slab. (U)

DREV R-4166/80 (UNCLASSIFIED)

Research and Development Branch, DND, Canada.
DREV, P.O. Box 880, Courcelette, Que. G0A 1R0

"A One-Dimensional Numerical Model of Laser Heating of Target Slabs"
by J.P. Morency

This report establishes a numerical scheme to solve the nonlinear one-dimensional heat transfer equation. The scheme is then applied to the case of laser-metals interaction and used to show the importance of thermo-physical properties variation on the temperature distribution within a slab. (U)

CRDV R-4166/80 (NON CLASSIFIE)

Bureau - Recherche et Développement, MDN, Canada
CRDV, C.P. 880, Courcelette, Qué. G0A 1R0

"Un modèle numérique unidimensionnel du chauffage d'une plaque métallique par laser" par J.P. Morency

Dans ce rapport on développe un schéma numérique de solution de l'équation unidimensionnelle non linéaire de conduction de la chaleur. On applique ensuite ce schéma à l'interaction laser-métaux et on montre l'importance de la variation des propriétés thermophysiques sur la distribution de la température dans une plaque métallique. (NC)

CRDV R-4166/80 (NON CLASSIFIE)

Bureau - Recherche et Développement, MDN, Canada
CRDV, C.P. 880, Courcelette, Qué. G0A 1R0

"Un modèle numérique unidimensionnel du chauffage d'une plaque métallique par laser" par J.P. Morency

Dans ce rapport on développe un schéma numérique de solution de l'équation unidimensionnelle non linéaire de conduction de la chaleur. On applique ensuite ce schéma à l'interaction laser-métaux et on montre l'importance de la variation des propriétés thermophysiques sur la distribution de la température dans une plaque métallique. (NC)

CRDV R-4166/80 (NON CLASSIFIE)

Bureau - Recherche et Développement, MDN, Canada
CRDV, C.P. 880, Courcelette, Qué. G0A 1R0

"Un modèle numérique unidimensionnel du chauffage d'une plaque métallique par laser" par J.P. Morency

Dans ce rapport on développe un schéma numérique de solution de l'équation unidimensionnelle non linéaire de conduction de la chaleur. On applique ensuite ce schéma à l'interaction laser-métaux et on montre l'importance de la variation des propriétés thermophysiques sur la distribution de la température dans une plaque métallique. (NC)

CRDV R-4166/80 (NON CLASSIFIE)

Bureau - Recherche et Développement, MDN, Canada
CRDV, C.P. 880, Courcelette, Qué. G0A 1R0

"Un modèle numérique unidimensionnel du chauffage d'une plaque métallique par laser" par J.P. Morency

Dans ce rapport on développe un schéma numérique de solution de l'équation unidimensionnelle non linéaire de conduction de la chaleur. On applique ensuite ce schéma à l'interaction laser-métaux et on montre l'importance de la variation des propriétés thermophysiques sur la distribution de la température dans une plaque métallique. (NC)